THE JOURNAL OF PHYSICAL CHEMISTRY Letters

Perspective

Cite This: J. Phys. Chem. Lett. 2018, 9, 5810−5821

pubs.acs.org/JPCL

Molecular Photon Upconversion Solar Cells Using Multilayer Assemblies: Progress and Prospects

Tristan Dilbeck and Kenneth Hanson*

Department of Chemistry & Biochemistry, Florida State University, Tallahassee, Florida 32306, United States

ABSTRACT: Molecular photon upconversion via triplet−triplet annihilation (TTA-UC) is an intriguing strategy to increase solar cell efficiencies and surpass the Shockley−Quiesser (SQ) limit. In this Perspective, we recount our group's efforts to harness TTA-UC by directly incorporating metal ion linked multilayers of acceptor and sensitizer molecules into an organic−inorganic hybrid solar cell architecture. These self-assembled multilayers facilitate both upconverted emission and photocurrent generation from the upconverted state with a record contribution of 0.158 mA cm^{-2} under 1 sun solar flux. We recount the progression toward this record and the mechanistic insights learned along the way, summarize the rate- and efficiency-limiting events, and outline improvements that must be made to produce a viable TTA-UC solar cell that can surpass the SQ limit. We also discuss the potential impact that efficient TTA-UC and photocurrent generation could have on existing record solar cells.

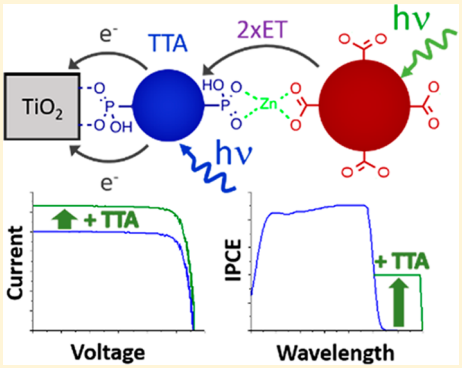

Molecular photon upconversion via triplet−triplet annihilation (TTA-UC)—combining two or more low-energy photons to generate a higher-energy excited state—is of interest for applications, including bioimaging, oxygen sensing, anticounterfeiting, and solar energy conversion, the focus of this Perspective.[1−10] TTA-UC, first observed in the 1960s,[11] is typically achieved using sensitizer and acceptor molecules with the mechanism summarized in Figure 1.[12] Briefly, low-energy

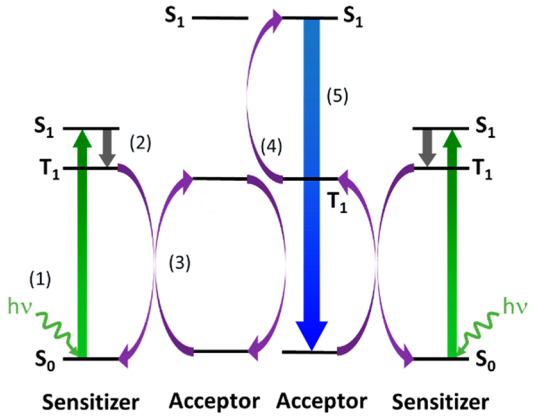

Figure 1. Mechanism for TTA-UC including (1) excitation, (2) intersystem crossing, (3) sensitizer-to-acceptor triplet energy transfer, (4) triplet−triplet annihilation, and (5) upconverted emission.

excitation of the sensitizer molecule into the singlet excited state, (1) in Figure 1, is followed by intersystem crossing to the triplet excited state manifold (2). The triplet excited-state energy is then transferred from the sensitizer to the acceptor molecule typically via a Dexter energy-transfer mechanism (3).[13,14] When two acceptor molecules in their triplet excited states are in proximity they can annihilate, with one acceptor relaxing back to its ground state and the other being promoted to its high-energy singlet excited state (4). Emission from the acceptor singlet excited state (5) is at a higher frequency than the excitation source, and thus the photon energy is upconverted in this process.

There are a number of strategies for combining sensitizer and acceptor molecules to facilitate TTA-UC, including in solution,[12,15−18] polymer films,[12,19−22] metal−organic frameworks,[23−26] as a neat solvent,[27,28] inside a microemulsion,[29] in a hydrogel,[30] and on surfaces.[31−41] In contrast to inorganic UC nanoparticles, which typically have relatively low efficiencies and require high excitation intensities (>1 W/cm^2),[7,11] molecular TTA is appealing because upconverted emission efficiencies upward of 60% have been demonstrated, and UC is achievable even under low-intensity irradiation (<10 mW/cm^2).[42−44] The latter point is particularly important in that TTA-UC can occur under subsolar intensities and thus has promise as a means of surpassing the Shockley−Queisser limit (~33%) for solar energy conversion.[45] Systems analysis indicates that using TTA-UC to harness previously transmitted, sub-band gap photons can increase the maximum theoretical solar cell efficiency from 33% to over 45%.[18,44,46,47]

TTA-UC is typically incorporated into solar energy conversion schemes via either optical[48−55] or electronic coupling arcitectures.[24,32,33,36,41,56] In the former, a TTA-UC film or solution is placed on the back side of a standard solar cell. The sub-band gap, low-energy light that is usually lost via transmission is then absorbed in the TTA-UC material, upconverted to supra-band gap energies, followed by emission

Received: August 26, 2018
Accepted: September 19, 2018
Published: September 19, 2018

DOI: 10.1021/acs.jpclett.8b02635
J. Phys. Chem. Lett. 2018, 9, 5810−5821

back to the solar cell. This strategy has the advantage of using established solar cell technologies, allowing each component to be independently optimized. One possible disadvantage is that, in contrast to the electronic coupling schemes (vide infra), the sensitizer concentration must be kept relatively low to prevent losses due to sensitizer−sensitizer annihilation, parasitic energy transfer, and/or inner filtering effects.[18] Additionally, because the UC emission is isotropic, this architecture requires reflectors or waveguides to direct the UC light to the solar cell to maximize TTA-UC harnessing efficiency.

In the electronically coupled scheme (also known as an integrated TTA-UC solar cell), TTA-UC is incorporated directly into the photocurrent generation mechanism. That is, following excitation and TTA, charge separation of the upconverted state occurs prior to UC emission. This scheme circumvents any issues with inner filtering losses, and thus sensitizer concentrations, and subsequent triplet excited state densities, can be increased even under low intensity light. However, this architecture does increase the complexity of the photocurrent generation mechanism and it requires the TTA-UC materials to be integrated into the excitation, exciton diffusion, charge separation, and electron/hole transport processes. While there have been a number of reports of optically coupled TTA-UC solar cells, perhaps this complexity is the reason why, prior to 2015, there were no examples of an electronically coupled TTA-UC solar cell.[31,41]

In 2015, our research group introduced self-assembled bilayers of sensitizer and acceptor molecules on a metal oxide substrate as a step toward an electronically coupled TTA-UC solar cell.[31] As shown in Figure 2a, self-assembled multilayers via metal ion linkages[57,58] are prepared through a stepwise soaking procedure.[59,60] Briefly, the high surface area metal oxide (ZrO_2 or TiO_2) is soaked in a solution of the acceptor molecule, then the Zn^{II} linking ion, and finally the sensitizer molecule. For our prototype films, 4,4′-(anthracene-9,10-diyl)bis(4,1-phenylene) diphosphonic acid (**A**) and Pt(II) meso-tetra(4-carboxyphenyl)porphine (**PtP**) were selected as the acceptor and sensitizer, respectively,[31] because they are derivatives of well-known upconversion pairs.[12,61] Each step of the film-formation process can be monitored using attenuated total reflection-infrared (ATR-IR)[62] and ultraviolet−visible (UV−vis) spectroscopy with the **PtP** concentration controlled by the soaking time. As can be seen in Figure 2c, absorption of the bilayer film (ZrO_2-**A**-Zn-**PtP**) is effectively the sum of its **A** and **PtP** components.

Under excitation with green light (532 nm), ZrO_2-**A**-Zn-**PtP** showed blue emission (380−520 nm) with a quantum yield of 0.0023 ± 0.0003 (Φ_{em} = photons out/photons in).[31] The emission intensity exhibited a quadratic-to-linear dependence on excitation intensity, indicating that the green-to-blue upconversion process is occurring via a TTA-UC mechanism.[63,64]

For photocurrent measurements, TiO_2 was used as the substrate because its conduction band energy is appropriate to act as an electron acceptor from the singlet excited state of **A** (^{1}**A***) but not the triplet excited state of **A** or **PtP** (^{3}**A*** or ^{3}**PtP***).[65,66] Under 2 sun irradiation (AM1.5) passed through a 495 nm long pass filter, a sandwich cell composed of a TiO_2-**A**-Zn-**PtP** working electrode, platinum counter electrode, and $TBAClO_4$ in MeCN electrolyte, had a peak photocurrent of 0.31 mA/cm^2.[31] Despite having the same total absorption, this photocurrent was three times the sum of its parts (TiO_2-**A** = 0.008 mA/cm^2 and TiO_2-**PtP** = 0.1 mA/cm^2). This observation, combined with the quadratic-to-linear-like intensity dependence, indicated that the bilayer film was an effective strategy not only to facilitate TTA-UC but also to charge separate the upconverted state. It is important to note that because of the lack of a regenerative redox mediator, the current was only transient and not sustained, but nonetheless it showed that charge separation of an upconverted state is feasible.

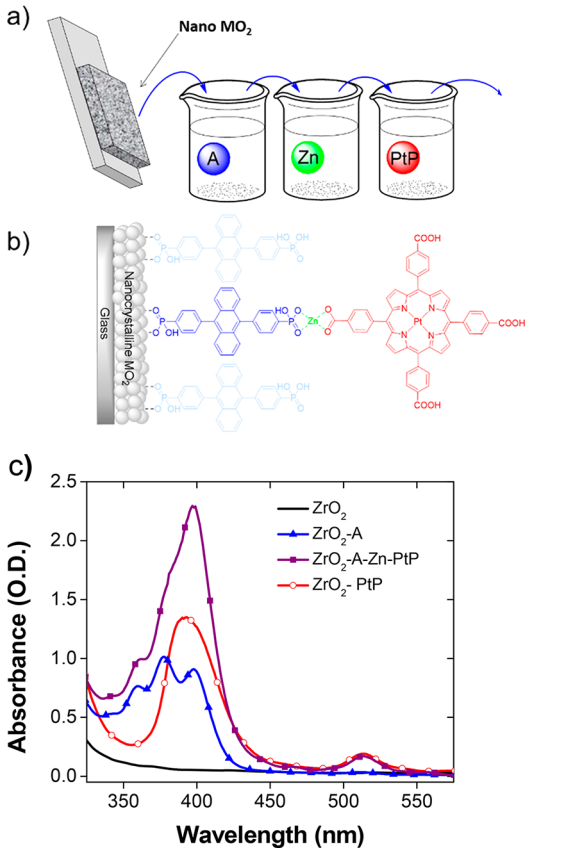

Figure 2. Preparation (a) and structure (b) of self-assembled bilayer on a nanocrystalline metal oxide substrate. (c) UV−vis absorption of the acceptor (blue), bilayer (purple), and sensitizer (red) films on ZrO_2 (black). Reproduced in part from ref 31. Copyright 2015 American Chemical Society.

This observation, combined with the quadratic-to-linear-like intensity dependence, indicated that the bilayer film was an effective strategy not only to facilitate TTA-UC but also to charge separate the upconverted state.

With a functioning TTA-UC film in hand we sought to determine the rate and efficiency of both the productive (green arrows in Figure 3) and nonproductive (red arrows in Figure 3) energy and electron-transfer events in the bilayer scheme.[34] Given the complexity of the system, simultaneously quantifying all dynamics events is an intractable task. Therefore, to determine the kinetics in the bilayer film, we used steady-state and time-resolved spectroscopy on a combination of

DOI: 10.1021/acs.jpclett.8b02635
J. Phys. Chem. Lett. 2018, 9, 5810−5821

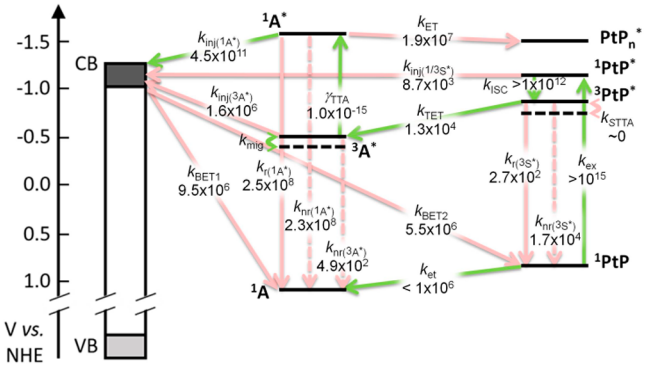

Figure 3. Productive (green) and nonproductive (red) processes that occur in a TTA-UC bilayer solar cell. All units are s^{-1} except for γ_{TTA} (cm^3 s^{-1}) (k_{ex} = excitation, k_{isc} = intersystem crossing, k_{STTA}= sensitizer−sensitizer triplet−triplet annihilation, $k_{r(3S^*)}$ = triplet sensitizer radiative decay, $k_{nr(3S^*)}$ = triplet sensitizer nonradiative decay, k_{TET} = sensitizer-to-acceptor triplet energy transfer, $k_{inj(1/3S^*)}$ = sensitizer electron injection, k_{et} = sensitizer-to-acceptor electron transfer, $k_{nr(3A^*)}$ = triplet acceptor nonradiative decay, γ_{TTA} = second-order triplet−triplet annihilation constant, $k_{r(1A^*)}$ = singlet acceptor radiative decay, $k_{nr(1A^*)}$ = singlet acceptor nonradiative decay, $k_{inj(1A^*)}$ = singlet acceptor electron injection, $k_{inj(3A^*)}$ = triplet acceptor electron injection, k_{BET1} = back electron transfer to acceptor, k_{BET2} = back electron transfer to sensitizer). Reprinted from ref 34. Copyright 2017 American Chemical Society.

substrates, sample and control monolayers and/or bilayers, and excitation wavelengths.

Radiative (k_r) and nonradiative (k_{nr}) decay constants, for example, were determined from the lifetime (τ) and emission quantum yield (Φ_{em}) for ZrO_2-**A** and ZrO_2-**PtP** using the equations $k_r = \Phi/\tau$ and $k_{nr} = (1 - \Phi)/\tau$. Other rate constants (e.g., k_{inj}, k_{BET}, etc.) could be quantified directly by monitoring the formation and disappearance of the oxidized dyes using transient absorption spectroscopy. For some events, where there are several competing decay processes, the rate constant must be determined using comparative measurements between samples. For example, sensitizer-to-acceptor triplet energy transfer (k_{TET}) is competitive with k_r, k_{nr}, and sensitizer−sensitizer annihilation (k_{STTA}). In this case, **PtP** emission lifetime from two different bilayer films, ZrO_2-**A**-Zn-**PtP** ($\tau_{s(bl)}$) and ZrO_2-**B**-Zn-**PtP** (τ_s), can be used to calculate k_{TET} using eq 1.

$$k_{TET} = \frac{1}{\tau_{s(bl)}} - \frac{1}{\tau_s} \quad (1)$$

In the latter sample, **B** is triphenyl-4,4′-diphosphonic acid,[34,60] a photochemically and photophysically inert surrogate of **A** that retains the bilayer structure but does not act as a TET acceptor. Because k_r, k_{nr}, and k_{STTA} are presumably similar for the two samples, the difference in **PtP** emission decay kinetics can be attributed to k_{TET}. From eq 1, a measured τ_s = 59 μs and $\tau_{s(bl)}$ = 33 μs results in a k_{TET} of 1.3 × 10^4 s^{-1}. The above three strategies were applied to determine a majority of the remaining rate constants.

Several notable observations can be made from the data in Figure 3. First, because of the relatively slow k_{TET} and competitive k_{nr}, the triplet energy-transfer yield is only ~30%. Thus, a 3-fold increase in TTA-UC efficiency, and photocurrent (vide infra), could be achieved if the interlayer energy-transfer rate is increased by an order of magnitude. Second, presumably because of the geometrically fixed nature of the bilayer assembly, nonproductive sensitizer−sensitizer annihilation does not occur ($k_{STTA} \approx 0$). Finally, electron injection from the acceptor singlet excited state happens on a picosecond time scale ($k_{inj(1A^*)} > 4.5 \times 10^{11}$ s^{-1}) and is significantly faster than nonproductive acceptor-to-sensitizer FRET. The negligible k_{STTA} and fast $k_{inj(1A^*)}$ are the primary reasons that the bilayer scheme can accommodate high sensitizer concentrations and not suffer the nonproductive losses that are typical in solution or heterogeneous TTA schemes.[15,18,67,68] The fast and near unity injection yield ($\Phi_{inj(1A^*)} \approx 100\%$) also indicates that the TTA-UC efficiency losses in the bilayer architecture are due to the steps prior to injection (i.e., slow cross surface migration and/or inefficient TTA).

Given the importance of sensitizer-to-acceptor TET and interacceptor, cross-surface energy transfer in dictating the TTA-UC efficiency, we then turned our attention toward understanding the role of the acceptor molecules' structure in dictating these dynamic events.[35,37] In addition to the change in energetics that has been observed in solution,[69−71] structural variations in the acceptor molecule also dictate intermolecular distance and relative orientation of the supramolecular assemblies which in turn influence TTA-UC rates and efficiencies. The acceptor molecules for our study were composed of an anthracene core functionalized with 9,10- or 2,6- phenyl, methyl, or directly bound phosphonic acid groups as depicted in Figure 4.

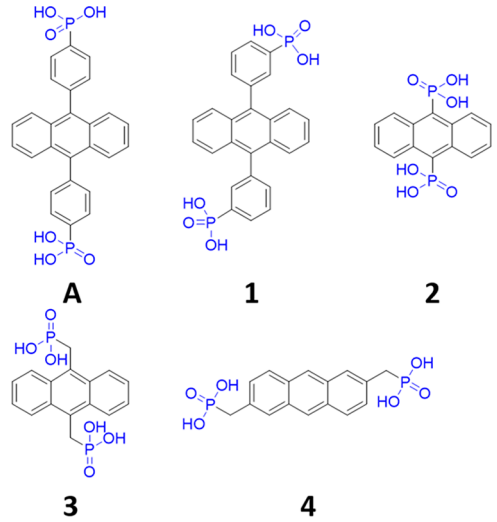

Figure 4. Structures of acceptor molecules **A** and **1**−**4** with metal ion binding PO_3H_2 groups highlighted in blue. Adapted with permission from ref 37. Copyright 2018 Royal Society of Chemistry.

All five anthracene derivatives form the bilayer film with **PtP** and adhere to isotherm loading behavior with a close packing, center-to-center distance (a_0) of 9−11 Å for dyes **A**, **1**, **3**, and **4** and 16 Å for **2**. As can be seen in Table 1, bilayers composed of **A** and **1**−**4** result in dramatically different Φ_{uc}, k_{FRET}, and triplet exciton diffusion rates.

Upon 532 nm excitation, all the ZrO_2-(**A**, **1**−**4**)-Zn-**PtP** films exhibit a blue emission feature from 420 to 500 nm with our prototype bilayer, ZrO_2-**A**-Zn-**PtP**, giving the highest quantum yield and then decreasing in the order **1** > **3** > **2** > **4**. Of the acceptor molecules, **2** exhibited the fastest sensitizer-to-acceptor interlayer triplet energy-transfer rate (k_{TET} = 2.1 × 10^4 s^{-1}). The higher rate and nearly doubled TET yield

DOI: 10.1021/acs.jpclett.8b02635
J. Phys. Chem. Lett. 2018, 9, 5810−5821

Table 1. UC Quantum Yield, Rates of TET and FRET, and Triplet Exciton Diffusion Coefficient for ZrO_2-(A, 1−4)-Zn-PtP in Deaerated MeCN

	Φ_{uc} [a]	k_{TET} (s^{-1}) [b]	k_{FRET} (s^{-1}) [c]	D ($cm^2\ s^{-1}$) [d]
A	0.0023	1.3×10^4	7.8×10^6	4.6×10^{-10}
1	0.0008	1.3×10^4	9.3×10^6	3.1×10^{-9}
2	0.0004	2.1×10^4	2.4×10^8	1.7×10^{-9}
3	0.0007	1.7×10^4	2.4×10^7	1.4×10^{-9}
4	0.0001	1.5×10^4	1.9×10^8	2.0×10^{-7}

[a]Measured relative to ZrO_2-**A**-Zn-**PtP** (Φ_{uc} = 0.0023) via actinometry. [b]$k_{TET} = 1/\tau_{s(bl)} - 1/\tau_{s.}$ [c]$k_{FRET} = 1/\tau_{A(bl)} - 1/\tau_{A.}$ [d]$D = \gamma_{TTA}/(8\pi a_0)$.

compared to **A** and **1** are presumably due, at least in part, to the lack of phenyl groups between the anthracene core and the phosphonate metal ion binding group, effectively decreasing the distance between **PtP** and **2**.

The rate of acceptor-to-sensitizer Förster resonance energy transfer (FRET) is dictated by the spectral overlap between emission and absorption (J), distance between the molecules, and the relative orientation of their transition dipole moments. Bilayers containing acceptor molecules **A** and **1** have similar J values (2.6×10^{-11} and 2.8×10^{-11} $cm^3\ M^{-1}$, respectively) and k_{FRET} suggesting that either the molecular orientations are similar, which is unlikely, or that differences in structure between these two bilayers play a diminished role in dictating FRET. In contrast, compound **4** exhibits the fastest (k_{FRET} = 1.86×10^8 s^{-1}) and most efficient (Φ_{FRET} = 0.58) FRET despite the 3 orders of magnitude lower J value (2.8×10^{-14} $cm^3\ M^{-1}$) relative to **A** and **1**−**3.** In this case, it is likely that the molecular orientations in ZrO_2-**4**-Zn-**PtP** are appropriate to strongly favor FRET.

From intensity-dependent emission measurements, the cross-surface triplet exciton diffusion constant (D) was calculated.[64] The origin of the 2 orders of magnitude higher D for **4** (2.0×10^{-7} $cm^2\ s^{-1}$) compared to the other acceptor molecules is currently unclear. One could envision that lower steric hindrance and/or the relative orientation dictated by the methyl groups at the 2,6- position would favor face-to-face stacking of the acceptor molecules.

Collectively these results demonstrate that the structure and orientation of the molecules in the bilayer, despite not being known, can have a profound impact on intra- and interlayer energy-transfer events. Measuring and modeling the structure at these interfaces will be a necessary step in fully explaining and then controlling migration, triplet energy transfer, back energy transfer, and ultimately the TTA-UC efficiency in self-assembled bilayer films.

Up until this point we have described only TTA-UC emission and transient photocurrent generation. To realize sustained photocurrent and a fully functional solar cell, an electron donor, $[Co(bpy)_3]^{2+/3+}$, was added to the electrolyte of our standard TiO_2-**A**-Zn-**PtP** electrochemical cell as depicted in Figure 5a.[32] Under 2 sun irradiation (2 × AM1.5) passed through a 495 nm long pass filter (Figure 5b), the sustained J_{sc} for TiO_2-**A**-Zn-**PtP** (0.028 ± 0.002 mA/cm^2) was more than 5 times greater than that of TiO_2-**PtP** (0.005 ± 0.002 mA/cm^2) and TiO_2-**A** (0.002 ± 0.002 mA/cm^2) devices.

Not only was there a dramatic increase in photocurrent relative to its monolayer components, but the J_{sc} showed a quadratic-to-linear dependence on excitation intensity, indicating that the photocurrent was the result of a TTA-UC mechanism.[63,64,72,73] As far as we know, this was only the second example of an integrated TTA-UC solar cell and the first observation of a quadratic-to-linear photocurrent−excitation intensity dependence.

The first example of an integrated TTA-UC solar cell was reported by Nattestad and co-workers[41] and was based on a heterogeneous TTA-UC scheme introduced by Morandeira and co-workers, where the acceptor was bound to the metal oxide surface and the sensitizer was in the electrolyte solution.[39,67] A comparison between the two architectures showed that for the hetergeneous scheme, there was first an increase and then a decrease in J_{sc} with respect to sensitizer concentration (Figure 6a), presumably because of non-productive sensitizer−sensitizer TTA losses at higher sensitizer concentration.[67] In contrast, the J_{sc} for the bilayer film (Figure 6b) continually increases up to the highest sensitizer loading concentration (**A**:**PtP**, 2:1) because, as noted above, the fixed geometry of the assembly inhibits k_{STTA}.[34]

Further photocurrent enhancements of 0.078 and 0.158 mA cm^{-2} were then achieved under 1 sun irradiation using multiple sensitizers in a self-assembled trilayer[33] and by changing the redox mediator,[36] respectively. In the former, the addition of a second sensitizer Pd(II) meso-tetra(4-carboxyphenyl)porphine (**PdP** in Figure 7a) in a TiO_2-**A**-Zn-**PdP**-Zn-**PtP** trilayer

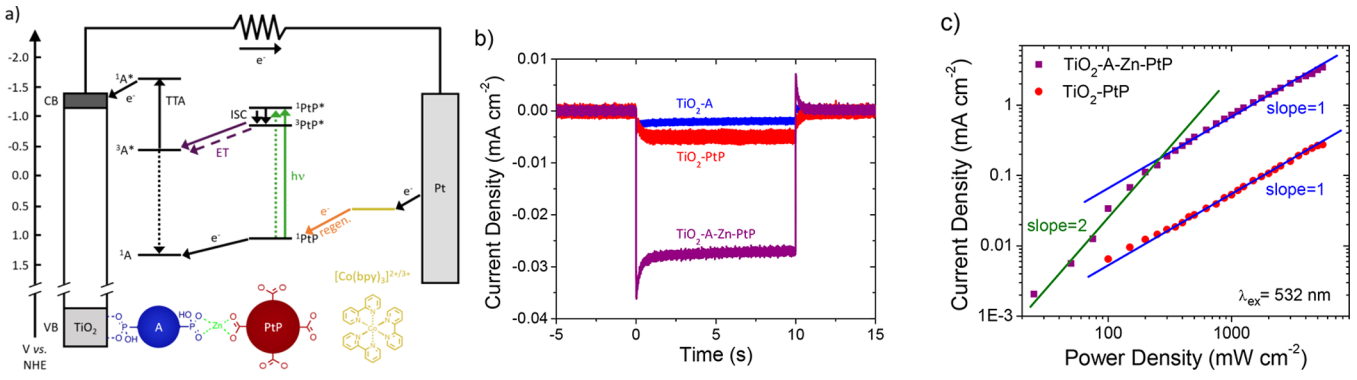

Figure 5. (a) Electronic transitions and energetics for TiO_2, **A**, **PtP**, and $[Co(bpy)_3]^{2+/3+}$ (vs NHE) in the TTA-UC solar cell. (b) Amperometric i−t curves for solar cells containing TiO_2-**A**, TiO_2-**PtP**, and TiO_2-**A**-Zn-**PtP** photoanodes with $[Co(bpy)_3]^{2+/3+}$ redox mediator under two equivalent AM1.5 solar irradiation. (c) Photocurrent density from TiO_2-**A**-Zn-**PtP** (purple) and TiO_2-**PtP** devices with respect to 532 nm excitation intensity. Reproduced in part from ref 32. Copyright 2016 American Chemical Society.

DOI: 10.1021/acs.jpclett.8b02635
J. Phys. Chem. Lett. 2018, 9, 5810−5821

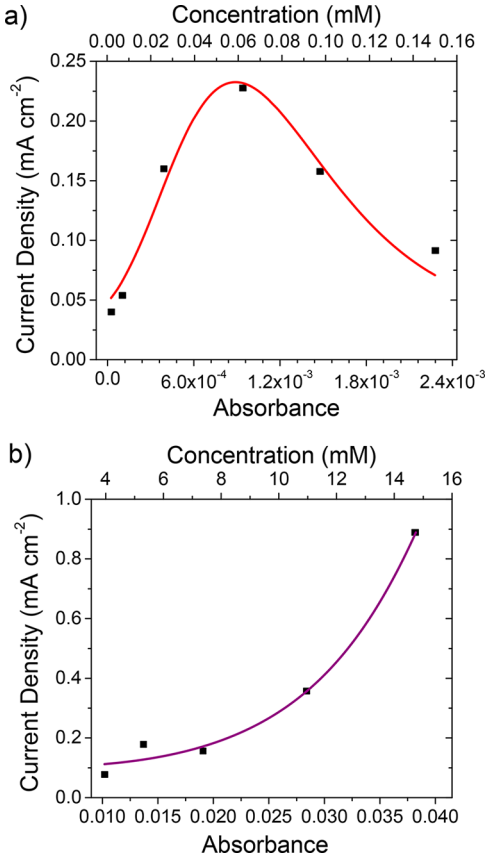

Figure 6. Photocurrent density at 0 V with respect to the absorbance at 532 nm (bottom) and sensitizer concentration (top) for (a) TiO_2-**A** with Pt(II) meso-tetraphenylporphine and $[Co(bpy)_3]^{2+/3+}$ in DMF and (b) TiO_2-**A**-Zn-**PtP** with $[Co(bpy)_3]^{2+/3+}$ in DMF and under 532 nm laser excitation (5.5 W/cm^2). Reprinted from ref 32. Copyright 2016 American Chemical Society.

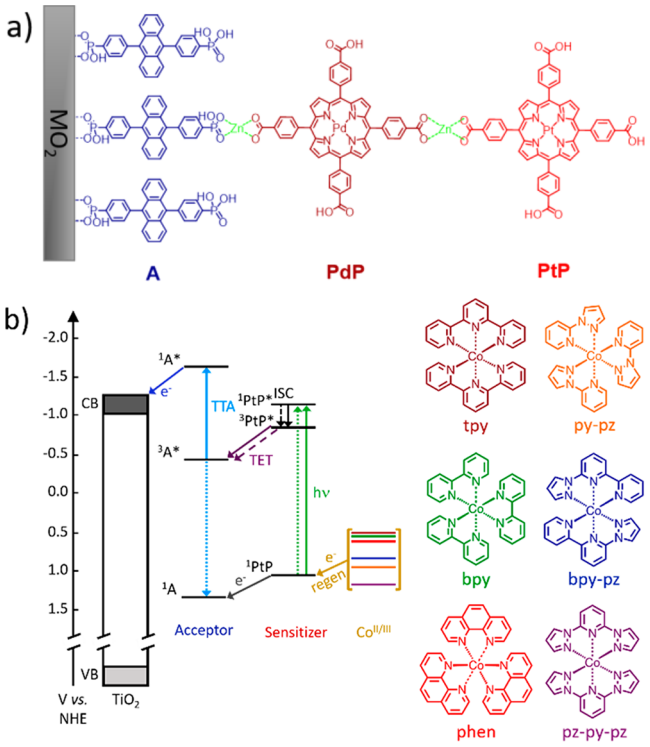

Figure 7. (a) Self-assembled trilayer on a nanocrystalline metal oxide substrate and (b) electronic transitions and energetics for TiO_2, **A**, **PtP**, and the mediators (vs NHE) alongside the structure of the $Co^{II/III}$ redox mediators (ISC, intersystem crossing; TET, triplet energy transfer; TTA, triplet−triplet annihilation). Reproduced in part from ref 36. Copyright 2017 American Chemical Society.

broadened and increased low-energy light absorption. The energetics were such that the triplet energy cascades from **PtP** to **PdP** to **A** effectively increasing the triplet densities on **A** which lowered the maximum TTA efficiency onset (I_{th} value) to sub-solar intensities (<1 mW/cm^2), effectively increasing the J_{sc} even under 1 sun flux.[15,51,74]

For the latter, it was found that the redox potential of the $Co^{2+/3+}$ mediator had a dramatic effect on J_{sc} and I_{th} values which varied over an order of magnitude across the six mediators (Figure 7b) with maximum and minimum values of 0.158 mA cm^{-2} and 0.8 mW/cm^2, respectively. Using transient absorption spectroscopy, we demonstrated that the cobalt mediator, while necessary for regenerating the dyes and closing the electrical circuit, can also quench the triplet excited states via (1) energy transfer or paramagnetic quenching by the Co^{II} species and (2) excited-state electron transfer to Co^{III} species.[36] This quenching reduces the acceptor triplet lifetime and is strongly competitive with TTA-UC, with some redox mediators quenching more than others. It is important to note that a J_{sc} of 0.158 mA cm^{-2} is the current record for harnessing TTA-UC in a solar cell and 0.8 mW/cm^2 is on par with the lowest I_{th} value reported for any TTA-UC system. From these results, it is clear that the choice of redox mediator plays a pivotal role in the efficiency of the device. The redox mediator must be chosen carefully to minimize recombination and excited-state quenching while maximizing dye regeneration.

It is important to note that a J_{sc} of 0.158 mA cm^{-2} is the current record for harnessing TTA-UC in a solar cell and 0.8 mW/cm^2 is on par with the lowest I_{th} value reported for any TTA-UC system.

To this point we have walked through our progression in understanding the dynamics of TTA-UC in a bilayer assembly as well as our efforts to harness UC in a solar cell. This work is a small contribution to the larger body of work that increasingly suggests the TTA-UC is a viable strategy for improving solar energy conversion efficiencies. Progress in the field to date, in terms of the J_{sc} contribution from TTA-UC (J_{UC}), corrected to the figure of merit under 1 sun conditions,[44,48] is shown in Figure 8.

This graph is an updated version of the one first introduced by Schmidt and co-workers.[44,55] In this graph, they define J_{UC}, and not open-circuit voltage (V_{oc}) or power conversion efficiency (PCE), as the critical metric to monitor while tracking progress in harnessing TTA-UC. This is justified given that TTA-UC is only a supplement to the high-energy, supra-band gap photoconversion components of the solar cell which will primarily dictate V_{oc} and PCE. It is also important to note that J_{UC} is the current density (mA cm^{-2}) divided by the square of the solar equivalent intensities used to excite the solar cell (i.e., mA cm^{-2} sun^{-2}). This figure of merit (FoM) approach[48,44,55] allows for a general comparison between cells

DOI: 10.1021/acs.jpclett.8b02635
J. Phys. Chem. Lett. 2018, 9, 5810−5821

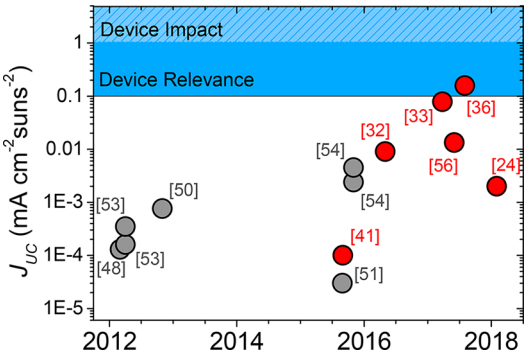

Figure 8. Progression in photocurrent contribution from TTA-UC (J_{UC}) with respect to time. Reference numbers are in brackets. Adapted from ref 44. Copyright 2017 American Chemical Society.

measured under different conditions. The underlying assumption is that solar cells measured under high intensities are operating in the quadratic regime, and thus dividing by the equivalent suns squared extrapolates to 1 sun conditions. For cells operating in the linear regime, this extrapolation will underestimate the performance under 1 sun conditions, and thus researchers are encouraged to measure and report TTA-UC solar cell performance under AM1.5 conditions.

They also defined a *device relevance threshold* of 0.1 mA/cm^2 that represents the minimum photocurrent generation necessary to make a notable impact on solar cell efficiencies. In Figure 8, optically and electronically coupled TTA-UC solar cells are depicted in gray and red, respectively. In addition to our bilayer solar cell work,[32,33,36] there are at least three other examples of integrated TTA-UC solar cells, including the heterogeneous device by Simpson et al. mentioned above (0.0001 mA cm^{-2}),[41] an OPV architecture by Lin et al. (0.0133 mA cm^{-2}),[56] and the MOF-based system of Ahmad et al. (0.002 mA cm^{-2}).[24]

A 1 mA/cm^2 contribution to current world record DSSC, OPV, or perovskite solar cells would increase PCEs by one percentage point or more.

With the development of new sensitizer pairs and TTA-UC architectures, much progress has been made toward reaching and surpassing the *device relevant threshold* (0.1 mA/cm^2). Here we propose the addition of a *device impact threshold* of 1 mA/cm^2. A 1 mA/cm^2 contribution to current world record DSSC, OPV, or perovskite solar cells would increase PCEs by one percentage point or more. In a research field where progress is made in intervals of tenths to hundredths of mA/cm^2, a 1 mA/cm^2 improvement would be a remarkable step forward. However, there is still much work to be done in not only generating 1 mA/cm^2 from TTA-UC but also coupling it to a world record solar cell.

In terms of improving performance from the bilayer TTA-UC solar cell, there are a number of steps that can and must be taken. Even with the current TiO_2-**A**-Zn-**PtP** bilayer and redox mediator, photocurrents greater than 0.158 mA cm^{-2} could be achieved through engineering strategies like optimizing film thicknesses and mediator concentrations,[75] inhibiting recombination using $TiCl_4$ treatments,[76] or better encapsulation to exclude or scavenge oxygen from the cell.[22,52,56,77,78] Additionally, as we described above, changing the redox mediator can have a profound effect on the J_{sc} and I_{th} values for TTA-UC.[36] Thus far we have studied only $Co^{2+/3+}$ complexes, but it is likely that a suitable mediator could be found that facilitates regeneration but would not quench the triplet excited state of the sensitizer and acceptor molecules. Organic solid-state hole-transporting materials[79] are particularly intriguing because they would not only lack any metal ion-based quenching mechanism but also help improve the long-term stability of the device and may help with oxygen exclusion.

The above strategies address issues that are extrinsic to the molecule−metal oxide interface, but the key to improving light harvesting and TTA-UC efficiency of the bilayer is by modifying the molecules in the assembly. One of the simplest steps forward is to change the sensitizer with the goals of increasing broad band absorption and reducing energy losses due to intersystem crossing. Os(II) coordination complexes,[80] quantum dots,[14,81,82] and thermally activated delayed fluorescence[83−85] sensitizers would all achieve this goal, but the latter two are particularly appealing as low-cost alternatives to Pt, Pd, or Os molecules.

Our previous work has shown that the structure of the molecules is also critical in dictating the rate and efficiency of TET, cross surface triplet migration,[35,37] and presumably TTA. Because the injection yield is near unity,[34] these steps are limiting TTA-UC in the bilayer, and improving any or all of them will increase solar energy conversion efficiencies. Unfortunately, while we know that the structure matters, there is currently no direct information about the intermolecular distances and orientations in the bilayer assembly. Techniques like near-edge X-ray absorption fine structure spectroscopy (NEXAFS),[86] sum-frequency generation,[87] two-photon photoelectron spectroscopy,[88] infrared reflection adsorption spectroscopy,[89] polarized Raman spectroscopy,[90] and ATR spectroscopy[91,92] will likely play a pivotal role in deciphering the bilayer structure at the interface. Understanding (1) how the position and type of surface/metal ion binding group dictates the structure and (2) how the structure influences the energy-transfer dynamics are two critical steps toward designing assemblies that favor energy transfer, migration, and TTA.

In both the optically and electronically coupled schemes, sub-band gap TTA-UC is a complement to supra-band gap absorption and solar energy conversion. In the optically coupled architecture, this is readily achieved using a TTA-UC filter/reflector in conjunction with a high-energy absorbing solar cell. For the integrated bilayer TTA-UC solar cell, we envision two possible strategies for harnessing both high- and low-energy light in a single-junction solar cell. The first is for the acceptor molecule to act as the high-energy absorber (i.e., direct excitation to the singlet state followed by electron injection). In our previous work, we showed that **A** in TiO_2-**A**-Zn-**PtP** can directly harness high-energy light via this mechanism (Figure 9a).[32] However, for this strategy to be useful, (1) the acceptor molecule must perform on par with the highest efficiency dyes used in world record DSSCs and (2) there must be no competitive high-energy absorption by the sensitizer molecule.

Regarding point one, finding a dye that has optimal properties for TTA (i.e., large singlet−triplet gap, fast intermolecular energy transfer, etc.) and photocurrent generation (i.e., broad-band absorption (300−700 nm), high

DOI: 10.1021/acs.jpclett.8b02635
J. Phys. Chem. Lett. 2018, 9, 5810−5821

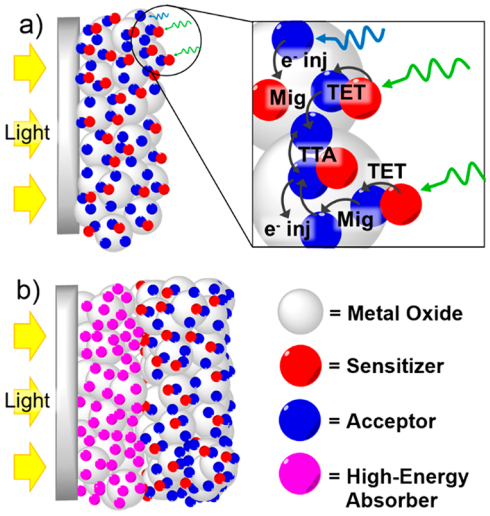

Figure 9. Two strategies to harness both high- and low-energy light on high surface area metal oxides (gray spheres) with the incident light depicted by yellow arrows. (a) Acceptor molecule (blue sphere) acts as both the high-energy absorber and acceptor from the sensitizer molecule (red sphere) in the TTA-UC mechanism (TET, triplet-energy transfer; mig, triplet migration; TTA, triplet−triplet annihilation; e^- inj, electron injection). (b) Layered TiO_2 anode with the high-energy absorber (purple sphere) and the TTA-UC molecules (red and blue spheres) spatially separated.

electron injection yield, fast regeneration, etc.) is a nontrivial, if not impossible task. Regarding point two, any high-energy absorption by the sensitizer molecule will result in J_{sc} losses because the TTA-UC mechanism is inherently less efficient (2 photons in 1 electron out) than direct excitation and electron injection (1 photon in 1 electron out). In an ideal scenario, the sensitizer would only absorb low-energy light (>700 nm) but have no optical transitions from 350 to 700 nm. As far as we know, no such sensitizer exists. That is not to say sensitizers and acceptors could not be found that have many of these properties, but an intensive cost-benefit analysis would be needed to see if the sacrifices in high-energy conversion are worth the gains from TTA-UC.

Arguably a more tangible solution may be to generate a layered TiO_2 anode as depicted in Figure 9b. In this architecture, the high-energy absorber and the TTA-UC portion are spatially separated on the bottom and top of the nanocrystalline metal oxide film, respectively. With the incident light from the bottom electrode, there are no concerns with competitive, high-energy absorption by the TTA-UC layer. Conceptually this strategy can be thought of as replacing the scattering layer of a record-breaking dye-sensitized or perovskite−TiO_2 solar cells with a TTA-UC layer. Layered dye-sensitized solar cells of this type have been demonstrated with complementary chromophores,[93,94] and we see no reason why these film formation strategies could not be used to generate a TTA-UC solar cell. One caveat is that the redox mediator or hole-transporting material would have to be appropriate for both the high- and low-energy conversion layers.

In terms of our bilayer TTA-UC solar cell, thus far we have only upconverted green light (500−550 nm) to blue light (400−500 nm), so our record photocurrents are not entirely *device relevant*, yet. Systems analyses indicate that maximum theoretical efficiencies of 45% can be realized only if low-energy UC is a supplement to a 1.76 eV (~700 nm) band gap, high-energy absorber. Given the limit $S_1 \geq 2 \times T_1$ and assuming no energy losses, TTA-UC could theoretically be used to harness 700−1400 nm (0.88−1.76 eV). In practice, however, this is a nontrivial task. In addition to inherent energy losses during energy- and electron-transfer events, the number of near-IR sensitizers is limited and the current low-energy excitation limit of TTA-UC is 980 nm (Φ_{TTA} = 0.01%).[80,81,95] The energy gap law (i.e., nonradiative rates exponentially increase as the energy gap decreases)[96,97] inherently limits the excited-state lifetime of near-IR sensitizer which can lower TET yields. Regardless, TTA-UC pairs nearing 1000 nm excitation exist and could be incorporated into the bilayer assembly. As we will show below, even absorption out to 1000 nm could have significant impacts on solar energy conversion efficiencies.

The ideal 1.76 eV band gap material (~700 nm) for optimal use of TTA-UC nicely coincides with the absorption onset of current world record DSSCs (~700 nm)[98] and perovskite (~800 nm) solar cells.[99] Assuming that we could replace their scattering layers with a TTA-UC layer, the question is, how much could we improve these solar cells? Figure 10 shows the results for a rough calculation on the possible contribution from TTA-UC to the highest-efficiency perovskite solar cell yet published.[99]

Numerous assumptions have gone into these calculations. The first is that the sensitizer has broad and uniform absorption from ~800−1000 nm. The second is regarding the efficiency of TTA. According to rigorous spin statistics, only 11% of triplet encounter pairs can undergo TTA.[100−103] If

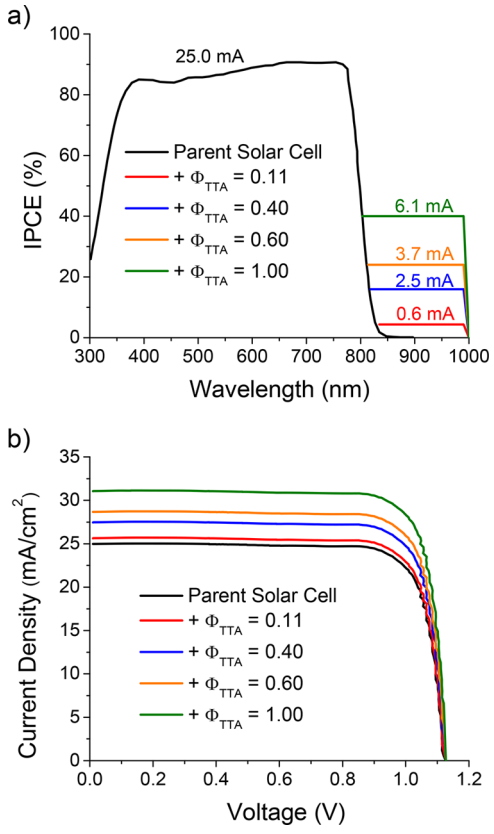

Figure 10. (a) IPCE and (b) *I*−*V* curve photocurrent enhancement by coupling TTA-UC to the solar cell in ref 99.

DOI: 10.1021/acs.jpclett.8b02635
J. Phys. Chem. Lett. 2018, 9, 5810−5821

the quintet encounter pairs are energetically inaccessible and the triplet pairs only result in the loss of one excited state, then secondary encounters would increase efficiencies up to 40%.[104] However, these limits are still in debate. With the common acceptor molecule rubrene, TTA-UC efficiencies upward of 60% have been observed.[43] TTA-UC could feasibly occur with 100% efficiency if the emitter is designed such that higher triplet energy levels are energetically inaccessible.[43,104] For example, singlet oxygen generation via triplet sensitization is a special type of triplet−triplet annihilation that can occur with 100% efficiency.[105]

Here we will perform the analysis with all of these possible scenarios (Φ_{TTA} = 0.11, 0.40, 0.60, 1.0), with two photons in giving one electron out (Φ_{TTA} = 0.11 gives 0.055 electrons per incident photon). Additionally, we will assume there is a 20% loss due to less than unity absorption, recombination losses, slow regeneration, etc. (i.e Φ_{TTA} = 1.0 gives an IPCE = (1.0/2 × 0.8) × 100% = 40%).

Using the resulting IPCE spectrum (Figure 10a) and the standard AM1.5 solar spectrum, the integrated TTA-UC photocurrent contribution (J_{UC}) from 800 to 1000 nm can be calculated. The $I-V$ curve for a perovskite solar cell, with contributions from each of these possible Φ_{TTA} scenarios, can then be simulated (Figure 10b) by adding J_{UC} to the J_{sc} and by assuming that the V_{oc}, series and shunt resistances, and fill factor remain unchanged. From the $I-V$ curves, the maximum power and PCEs can be calculated, and the results are summarized in Table 2.

Table 2. PCE Enhancements for a Perovskite Solar Cell Supplemented by TTA-UC from 800 to 1000 nm with Various Φ_{TTA} Values

Φ_{TTA}	IPCE$_{TTA}$ (%)[a]	J_{UC} (mA/cm^2)[b]	PCE w/UC (%)[c]
0	0	0	22.2[d]
0.11	4.4	0.6	22.7
0.40	16	2.5	24.3
0.60	24	3.7	25.4
1.00	40	6.1	27.6

[a]Calculated from (Φ_{TTA}/2 × 0.8) × 100 [b]Integrated current from 800 to 1000 nm using the IPCE from column two.[106] [c]Calculated from the $I-V$ curve generated by adding J_{UC} to the record J_{sc} (25.0 mA cm^{-2}) and assuming that the V_{oc} (1.10 V), series and shunt resistances, and FF (0.805) remain unchanged. [d]From ref 99.

For 100% efficient TTA-UC, there is a remarkable J_{UC} of 6.1 mA/cm^2 and an increase in solar cell efficiency of 5.4 percentage points.

Even for the spin statistically limited scenario (Φ_{TTA} = 0.11), there is a J_{UC} of 0.6 mA/cm^2 and an increase in solar cell efficiency by 0.5 percentage points. For 100% efficient TTA-UC, there is a remarkable J_{UC} of 6.1 mA/cm^2 and an increase in solar cell efficiency of 5.4 percentage points. The assumed 20% loss is readily achievable in a standard solar cell but may be generous for a TTA-UC device because of the additional loss pathways noted above (i.e., quenching by the mediator, inner filtering losses, etc.). That said, with a reasonable Φ_{TTA} of 0.40, a *device impact threshold* of 1 mA/cm^2 can be achieved even with 70% non-TTA photon-to-current losses. It is also worth noting that the band gap of this perovskite solar cell (~1.5 eV) is not ideal to maximize the efficiency enhancement from TTA.[99] An increased V_{oc}, J_{UC} contribution, and overall conversion efficiency could be achieved with a 1.76 eV (~700 nm) band gap perovskite solar cell. Alternatively, given its lower efficiency and higher-energy onset, the TTA-UC contribution would be larger for the world record DSSC.[98]

These results of course are optimistic in that we assume that the addition of TTA-UC in no way hinders the performance of the record solar cell. While that may be the case with the TTA-UC filter strategy, it most certainly will not be true for an integrated TTA-UC solar cell. Additionally, while Φ_{TTA} greater than 11% under 1 sun flux have been demonstrated with visible TTA-UC,[43] the record Φ_{TTA} with 980 nm excitation is only 0.01% and requires >10 W/cm^2 excitation source,[81] well above solar flux (<10 mA/cm^2). Nonetheless, these calculations show that TTA-UC could make major contributions to solar energy conversion but only after significant advances in (1) coupling TTA-UC to record-breaking solar cells, (2) shifting absorption to 1000 nm, and (3) increasing TTA-UC efficiencies under 1 sun conditions.

In this Perspective we have discussed our progress facilitating and harnessing TTA-UC using self-assembled bilayers of sensitizer and acceptor molecules on a metal oxide substrate. These bilayers are effective in facilitating TTA-UC emission and charge separation of the UC state. Kinetic analysis of the TTA-UC mechanism shows the triplet energy-transfer and TTA events, but not sensitizer−sensitizer TTA or electron injection, are fundamentally limiting the TTA-UC efficiency of the current bilayer film. The structure of the acceptor molecule, the addition of a second sensitizer, and variation of the redox mediator can all have a profound effect on the rate and efficiency of energy transfer, TTA-UC, and photocurrent generation. Using this knowledge, a TTA-UC photocurrent of up to 0.158 mA cm^{-2} has been achieved and is the current record for harnessing TTA-UC in a solar cell. We also discuss where progress needs to be made to improve TTA-UC in the bilayer, including (1) understanding and controlling the bilayer structure, (2) incorporating new redox mediators and sensitizers, (3) coupling the bilayer to world record solar cells, and (4) shifting TTA-UC bilayer absorption into the near-IR. We close by performing rough calculations as to what the contribution of TTA-UC to a world record solar cells could be. In totality, this work shows that while significant progress has been achieved, there is still much progress to be made in increasing the efficiency and harnessing TTA-UC for efficient solar energy conversion.

AUTHOR INFORMATION

Corresponding Author

*E-mail: hanson@chem.fsu.edu.

ORCID

Kenneth Hanson: 0000-0001-7219-7808

Notes

The authors declare no competing financial interest.

Biographies

Tristan Dilbeck received her B.S. in Chemistry from California Polytechnic State University, San Luis Obispo in 2014 and then entered graduate school at Florida State University where she joined the lab of Dr. Kenneth Hanson. Her research focuses on measuring

DOI: 10.1021/acs.jpclett.8b02635
J. Phys. Chem. Lett. 2018, 9, 5810−5821

energy- and electron-transfer dynamics of photon upconversion in bilayer films as well as in other systems.

Kenneth Hanson received a B.S. in Chemistry from Saint Cloud State University (2005) and his Ph.D. from the University of Southern California (2010); this was followed by an appointment as a postdoctoral scholar at the University of North Carolina at Chapel Hill (2010−2013). His independent research career began in 2013 at Florida State University where his research focuses on design, synthesis, and characterization of photoactive molecules and materials for applications including catalysis and solar energy conversion.

■ ACKNOWLEDGMENTS

The authors thank the Florida State University's Energy and Materials Initiative for facilitating aspects of this research. Some of this material is based upon work supported by the National Science Foundation under Grant No. DMR-1752782.

■ REFERENCES

(1) Zhang, P.; Steelant, W.; Kumar, M.; Scholfield, M. Versatile Photosensitizers for Photodynamic Therapy at Infrared Excitation. *J. Am. Chem. Soc.* **2007**, *129*, 4526−4527.
(2) Khnayzer, R. S.; Blumhoff, J.; Harrington, J. A.; Haefele, A.; Deng, F.; Castellano, F. N. Upconversion-powered photoelectrochemistry. *Chem. Commun.* **2012**, *48*, 209−211.
(3) Kim, J.-H.; Kim, J.-H. Encapsulated Triplet−Triplet Annihilation-Based Upconversion in the Aqueous Phase for Sub-Band-Gap Semiconductor Photocatalysis. *J. Am. Chem. Soc.* **2012**, *134*, 17478−17481.
(4) Jiang, Z.; Xu, M.; Li, F.; Yu, Y. Red-Light-Controllable Liquid-Crystal Soft Actuators via Low-Power Excited Upconversion Based on Triplet−Triplet Annihilation. *J. Am. Chem. Soc.* **2013**, *135*, 16446−16453.
(5) McCusker, C. E.; Castellano, F. N. Materials Integrating Photochemical Upconversion. *Top. Curr. Chem.* **2016**, *374*, 19.
(6) Hagstrom, A. L.; Lee, H.-L.; Lee, M.-S.; Choe, H.-S.; Jung, J.; Park, B.-G.; Han, W.-S.; Ko, J.-S.; Kim, J.-H.; Kim, J.-H. Flexible and Micropatternable Triplet−Triplet Annihilation Upconversion Thin Films for Photonic Device Integration and Anticounterfeiting Applications. *ACS Appl. Mater. Interfaces* **2018**, *10*, 8985−8992.
(7) Zhou, J.; Liu, Q.; Feng, W.; Sun, Y.; Li, F. Upconversion Luminescent Materials: Advances and Applications. *Chem. Rev.* **2015**, *115*, 395−465.
(8) Askes, S. H. C.; Mora, N. L.; Harkes, R.; Koning, R. I.; Koster, B.; Schmidt, T.; Kros, A.; Bonnet, S. Imaging the lipid bilayer of giant unilamellar vesicles using red-to-blue light upconversion. *Chem. Commun.* **2015**, *51*, 9137−9140.
(9) Borisov, S. M.; Larndorfer, C.; Klimant, I. Triplet−Triplet Annihilation-Based Anti-Stokes Oxygen Sensing Materials with a Very Broad Dynamic Range. *Adv. Funct. Mater.* **2012**, *22*, 4360−4368.
(10) Pedrini, J.; Monguzzi, A. Recent Advances in the Application Triplet−Triplet Annihilation-Based Photon Upconversion Systems to Solar Technologies. *J. Photonics Energy* **2018**, *8*, 1.
(11) Auzel, F. Upconversion and Anti-Stokes Processes with f and d Ions in Solids. *Chem. Rev.* **2004**, *104*, 139−174.
(12) Singh-Rachford, T. N.; Castellano, F. N. Photon upconversion based on sensitized triplet−triplet annihilation. *Coord. Chem. Rev.* **2010**, *254*, 2560−2573.
(13) Dexter, D. L. A Theory of Sensitized Luminescence in Solids. *J. Chem. Phys.* **1953**, *21*, 836−850.
(14) Mongin, C.; Garakyaraghi, S.; Razgoniaeva, N.; Zamkov, M.; Castellano, F. N. Direct observation of triplet energy transfer from semiconductor nanocrystals. *Science* **2016**, *351*, 369−372.
(15) Baluschev, S.; Yakutkin, V.; Wegner, G.; Miteva, T.; Nelles, G.; Yasuda, A.; Chernov, S.; Aleshchenkov, S.; Cheprakov, A. Upconversion with ultrabroad excitation band: Simultaneous use of two sensitizers. *Appl. Phys. Lett.* **2007**, *90*, 181103.
(16) Kozlov, D. V.; Castellano, F. N. Anti-Stokes delayed fluorescence from metal−organic bichromophores. *Chem. Commun.* **2004**, 2860−2861.
(17) Baluschev, S.; Miteva, T.; Yakutkin, V.; Nelles, G.; Yasuda, A.; Wegner, G. Up-Conversion Fluorescence: Noncoherent Excitation by Sunlight. *Phys. Rev. Lett.* **2006**, *97*, 143903.
(18) Baluschev, S.; Yakutkin, V.; Miteva, T.; Wegner, G.; Roberts, T.; Nelles, G.; Yasuda, A.; Chernov, S.; Aleshchenkov, S.; Cheprakov, A. A general approach for non-coherently excited annihilation up-conversion: transforming the solar-spectrum. *New J. Phys.* **2008**, *10*, 013007.
(19) Islangulov, R. R.; Lott, J.; Weder, C.; Castellano, F. N. Noncoherent Low-Power Upconversion in Solid Polymer Films. *J. Am. Chem. Soc.* **2007**, *129*, 12652−12653.
(20) Boutin, P. C.; Ghiggino, K. P.; Kelly, T. L.; Steer, R. P. Photon Upconversion by Triplet−Triplet Annihilation in Ru(bpy)3- and DPA-Functionalized Polymers. *J. Phys. Chem. Lett.* **2013**, *4*, 4113−4118.
(21) Thévenaz, D. C.; Lee, S. H.; Guignard, F.; Balog, S.; Lattuada, M.; Weder, C.; Simon, Y. C. Single-Component Upconverting Polymeric Nanoparticles. *Macromol. Rapid Commun.* **2016**, *37*, 826−832.
(22) Di, D.; Yang, L.; Richter, J. M.; Meraldi, L.; Altamimi, R. M.; Alyamani, A. Y.; Credgington, D.; Musselman, K. P.; MacManus-Driscoll, J. L.; Friend, R. H. Efficient Triplet Exciton Fusion in Molecularly Doped Polymer Light-Emitting Diodes. *Adv. Mater.* **2017**, *29*, 1605987.
(23) Oldenburg, M.; Turshatov, A.; Busko, D.; Wollgarten, S.; Adams, M.; Baroni, N.; Welle, A.; Redel, E.; Wöll, C.; Richards, B. S.; Howard, I. A. Photon Upconversion at Crystalline Organic−Organic Heterojunctions. *Adv. Mater.* **2016**, *28*, 8477−8482.
(24) Ahmad, S.; Liu, J.; Gong, C.; Zhao, J.; Sun, L. Photon Up-Conversion via Epitaxial Surface-Supported Metal−Organic Framework Thin Films with Enhanced Photocurrent. *ACS Appl. Energy Mater.* **2018**, *1*, 249−253.
(25) Rowe, J. M.; Zhu, J.; Soderstrom, E. M.; Xu, W.; Yakovenko, A.; Morris, A. J. Sensitized photon upconversion in anthracene-based zirconium metal−organic frameworks. *Chem. Commun.* **2018**, *54*, 7798−7801.
(26) Amemori, S.; Gupta, R. K.; Böhm, M. L.; Xiao, J.; Huynh, U.; Oyama, T.; Kaneko, K.; Rao, A.; Yanai, N.; Kimizuka, N. Hybridizing semiconductor nanocrystals with metal−organic frameworks for visible and near-infrared photon upconversion. *Dalton Trans* **2018**, *47*, 8590−8594.
(27) Duan, P.; Yanai, N.; Kimizuka, N. Photon Upconverting Liquids: Matrix-Free Molecular Upconversion Systems Functioning in Air. *J. Am. Chem. Soc.* **2013**, *135*, 19056−19059.
(28) Duan, P.; Yanai, N.; Nagatomi, H.; Kimizuka, N. Photon Upconversion in Supramolecular Gel Matrixes: Spontaneous Accumulation of Light-Harvesting Donor−Acceptor Arrays in Nanofibers and Acquired Air Stability. *J. Am. Chem. Soc.* **2015**, *137*, 1887−1894.
(29) Penconi, M.; Gentili, P. L.; Massaro, G.; Elisei, F.; Ortica, F. A triplet-triplet annihilation based up-conversion process investigated in homogeneous solutions and oil-in-water microemulsions of a surfactant. *Photochem. Photobiol. Sci.* **2014**, *13*, 48−61.
(30) Bharmoria, P.; Hisamitsu, S.; Nagatomi, H.; Ogawa, T.; Morikawa, M.-a.; Yanai, N.; Kimizuka, N. Simple and Versatile Platform for Air-Tolerant Photon Upconverting Hydrogels by Biopolymer−Surfactant−Chromophore Co-assembly. *J. Am. Chem. Soc.* **2018**, *140*, 10848.
(31) Hill, S. P.; Banerjee, T.; Dilbeck, T.; Hanson, K. Photon Upconversion and Photocurrent Generation via Self-Assembly at Organic−Inorganic Interfaces. *J. Phys. Chem. Lett.* **2015**, *6*, 4510−4517.
(32) Hill, S. P.; Dilbeck, T.; Baduell, E.; Hanson, K. Integrated Photon Upconversion Solar Cell via Molecular Self-Assembled Bilayers. *ACS Energy Lett.* **2016**, *1*, 3−8.

DOI: 10.1021/acs.jpclett.8b02635
J. Phys. Chem. Lett. 2018, 9, 5810−5821

(33) Dilbeck, T.; Hill, S. P.; Hanson, K. Harnessing molecular photon upconversion at sub-solar irradiance using dual sensitized self-assembled trilayers. *J. Mater. Chem. A* **2017**, *5*, 11652−11660.
(34) Dilbeck, T.; Wang, J. C.; Zhou, Y.; Olsson, A.; Sykora, M.; Hanson, K. Elucidating the Energy- and Electron-Transfer Dynamics of Photon Upconversion in Self-Assembled Bilayers. *J. Phys. Chem. C* **2017**, *121*, 19690−19698.
(35) Zhou, Y.; Hill, S. P.; Hanson, K. Influence of meta- and para-phosphonated diphenylanthracene on photon upconversion in self-assembled bilayers. *J. Photonics Energy* **2018**, *8*, 1.
(36) Hill, S. P.; Hanson, K. Harnessing Molecular Photon Upconversion in a Solar Cell at Sub-solar Irradiance: Role of the Redox Mediator. *J. Am. Chem. Soc.* **2017**, *139*, 10988−10991.
(37) Zhou, Y.; Ayad, S.; Ruchlin, C.; Posey, V.; Hill, S. P.; Wu, Q.; Hanson, K. Examining the Role of Acceptor Molecule Structure in Self-Assembled Bilayers: Surface Loading, Stability, Energy Transfer, and Upconverted Emission. *Phys. Chem. Chem. Phys.* **2018**, *20*, 20513−20524.
(38) Lissau, J. S.; Gardner, J. M.; Morandeira, A. Photon Upconversion on Dye-Sensitized Nanostructured ZrO2 Films. *J. Phys. Chem. C* **2011**, *115*, 23226−23232.
(39) Lissau, J. S.; Nauroozi, D.; Santoni, M.-P.; Ott, S.; Gardner, J. M.; Morandeira, A. Anchoring Energy Acceptors to Nanostructured ZrO2 Enhances Photon Upconversion by Sensitized Triplet−Triplet Annihilation Under Simulated Solar Flux. *J. Phys. Chem. C* **2013**, *117*, 14493−14501.
(40) Lissau, J. S.; Nauroozi, D.; Santoni, M.-P.; Ott, S.; Gardner, J. M.; Morandeira, A. Photon Upconversion from Chemically Bound Triplet Sensitizers and Emitters on Mesoporous ZrO2: Implications for Solar Energy Conversion. *J. Phys. Chem. C* **2015**, *119*, 25792−25806.
(41) Simpson, C.; Clarke, T. M.; MacQueen, R. W.; Cheng, Y. Y.; Trevitt, A. J.; Mozer, A. J.; Wagner, P.; Schmidt, T. W.; Nattestad, A. An intermediate band dye-sensitised solar cell using triplet-triplet annihilation. *Phys. Chem. Chem. Phys.* **2015**, *17*, 24826−24830.
(42) Tayebjee, M. J. Y.; McCamey, D. R.; Schmidt, T. W. Beyond Shockley−Queisser: Molecular Approaches to High-Efficiency Photovoltaics. *J. Phys. Chem. Lett.* **2015**, *6*, 2367−2378.
(43) Cheng, Y. Y.; Fückel, B.; Khoury, T.; Clady, R. G. C. R.; Tayebjee, M. J. Y.; Ekins-Daukes, N. J.; Crossley, M. J.; Schmidt, T. W. Kinetic Analysis of Photochemical Upconversion by Triplet−Triplet Annihilation: Beyond Any Spin Statistical Limit. *J. Phys. Chem. Lett.* **2010**, *1*, 1795−1799.
(44) Frazer, L.; Gallaher, J. K.; Schmidt, T. W. Optimizing the Efficiency of Solar Photon Upconversion. *ACS Energy Lett.* **2017**, *2*, 1346−1354.
(45) Shockley, W.; Queisser, H. J. Detailed Balance Limit of Efficiency of p-n Junction Solar Cells. *J. Appl. Phys.* **1961**, *32*, 510−519.
(46) Trupke, T.; Green, M. A.; Würfel, P. Improving solar cell efficiencies by up-conversion of sub-band-gap light. *J. Appl. Phys.* **2002**, *92*, 4117−4122.
(47) Ekins-Daukes, N. J.; Schmidt, T. W. A molecular approach to the intermediate band solar cell: The symmetric case. *Appl. Phys. Lett.* **2008**, *93*, 063507.
(48) Cheng, Y. Y.; Fuckel, B.; MacQueen, R. W.; Khoury, T.; Clady, R. G. C. R.; Schulze, T. F.; Ekins-Daukes, N. J.; Crossley, M. J.; Stannowski, B.; Lips, K.; Schmidt, T. W. Improving the light-harvesting of amorphous silicon solar cells with photochemical upconversion. *Energy Environ. Sci.* **2012**, *5*, 6953−6959.
(49) Nattestad, A.; Cheng, Y. Y.; MacQueen, R. W.; Schulze, T. F.; Thompson, F. W.; Mozer, A. J.; Fückel, B.; Khoury, T.; Crossley, M. J.; Lips, K.; Wallace, G. G.; Schmidt, T. W. Dye-Sensitized Solar Cell with Integrated Triplet−Triplet Annihilation Upconversion System. *J. Phys. Chem. Lett.* **2013**, *4*, 2073−2078.
(50) Schulze, T. F.; Cheng, Y. Y.; Fückel, B.; MacQueen, R. W.; Danos, A.; Davis, N. J. L. K.; Tayebjee, M. J. Y.; Khoury, T.; Clady, R. G. C. R.; Ekins-Daukes, N. J.; Crossley, M. J.; Stannowski, B.; Lips, K.; Schmidt, T. W. Photochemical Upconversion Enhanced Solar Cells: Effect of a Back Reflector. *Aust. J. Chem.* **2012**, *65*, 480−485.
(51) Monguzzi, A.; Borisov, S. M.; Pedrini, J.; Klimant, I.; Salvalaggio, M.; Biagini, P.; Melchiorre, F.; Lelii, C.; Meinardi, F. Efficient Broadband Triplet−Triplet Annihilation-Assisted Photon Upconversion at Subsolar Irradiance in Fully Organic Systems. *Adv. Funct. Mater.* **2015**, *25*, 5617−5624.
(52) Li, C.; Koenigsmann, C.; Deng, F.; Hagstrom, A.; Schmuttenmaer, C. A.; Kim, J.-H. Photocurrent Enhancement from Solid-State Triplet−Triplet Annihilation Upconversion of Low-Intensity, Low-Energy Photons. *ACS Photonics* **2016**, *3*, 784−790.
(53) Schulze, T. F.; Czolk, J.; Cheng, Y.-Y.; Fückel, B.; MacQueen, R. W.; Khoury, T.; Crossley, M. J.; Stannowski, B.; Lips, K.; Lemmer, U.; Colsmann, A.; Schmidt, T. W. Efficiency Enhancement of Organic and Thin-Film Silicon Solar Cells with Photochemical Upconversion. *J. Phys. Chem. C* **2012**, *116*, 22794−22801.
(54) Cheng, Y. Y.; Nattestad, A.; Schulze, T. F.; MacQueen, R. W.; Fuckel, B.; Lips, K.; Wallace, G. G.; Khoury, T.; Crossley, M. J.; Schmidt, T. W. Increased upconversion performance for thin film solar cells: a trimolecular composition. *Chem. Sci.* **2016**, *7*, 559−568.
(55) Cheng, Y. Y.; Fückel, B.; Schulze, T.; MacQueen, R. W.; Tayebjee, M. J. Y.; Danos, A.; Khoury, T.; Clady, R. G. C. R.; Ekins-Daukes, N. J.; Crossley, M. J.; Stannowski, B.; Lips, K.; Schmidt, T. W. Improving the light-harvesting of second generation solar cells with photochemical upconversion; Proceedings of SPIE Organic Photonics + Electronics; SPIE, 2012; p 3.
(56) Lin, Y. L.; Koch, M.; Brigeman, A. N.; Freeman, D. M. E.; Zhao, L.; Bronstein, H.; Giebink, N. C.; Scholes, G. D.; Rand, B. P. Enhanced sub-bandgap efficiency of a solid-state organic intermediate band solar cell using triplet-triplet annihilation. *Energy Environ. Sci.* **2017**, *10*, 1465−1475.
(57) Terada, K.; Kobayashi, K.; Hikita, J.; Haga, M.-a. Electric Conduction Properties of Self-assembled Monolayer Films of Ru Complexes with Disulfide/Phosphonate Anchors in a Au-(Molecular Ensemble)-(Au Nanoparticle) Junction. *Chem. Lett.* **2009**, *38*, 416−417.
(58) Lee, H.; Kepley, L. J.; Hong, H. G.; Mallouk, T. E. Inorganic analogs of Langmuir-Blodgett films: adsorption of ordered zirconium 1,10-decanebisphosphonate multilayers on silicon surfaces. *J. Am. Chem. Soc.* **1988**, *110*, 618−620.
(59) Hanson, K.; Torelli, D. A.; Vannucci, A. K.; Brennaman, M. K.; Luo, H.; Alibabaei, L.; Song, W.; Ashford, D. L.; Norris, M. R.; Glasson, C. R. K.; Concepcion, J. J.; Meyer, T. J. Self-Assembled Bilayer Films of Ruthenium(II)/Polypyridyl Complexes through Layer-by-Layer Deposition on Nanostructured Metal Oxides. *Angew. Chem., Int. Ed.* **2012**, *51*, 12782−12785.
(60) Wang, J. C.; Murphy, I. A.; Hanson, K. Modulating Electron Transfer Dynamics at Dye−Semiconductor Interfaces via Self-Assembled Bilayers. *J. Phys. Chem. C* **2015**, *119*, 3502−3508.
(61) Gray, V.; Dzebo, D.; Abrahamsson, M.; Albinsson, B.; Moth-Poulsen, K. Triplet-triplet annihilation photon-upconversion: towards solar energy applications. *Phys. Chem. Chem. Phys.* **2014**, *16*, 10345−10352.
(62) Gao, W.; Dickinson, L.; Grozinger, C.; Morin, F. G.; Reven, L. Self-Assembled Monolayers of Alkylphosphonic Acids on Metal Oxides. *Langmuir* **1996**, *12*, 6429−6435.
(63) Haefele, A.; Blumhoff, J.; Khnayzer, R. S.; Castellano, F. N. Getting to the (Square) Root of the Problem: How to Make Noncoherent Pumped Upconversion Linear. *J. Phys. Chem. Lett.* **2012**, *3*, 299−303.
(64) Monguzzi, A.; Mezyk, J.; Scotognella, F.; Tubino, R.; Meinardi, F. Upconversion-induced fluorescence in multicomponent systems: Steady-state excitation power threshold. *Phys. Rev. B: Condens. Matter Mater. Phys.* **2008**, *78*, 195112.
(65) Qu, P.; Meyer, G. J. Proton-Controlled Electron Injection from Molecular Excited States to the Empty States in Nanocrystalline TiO2. *Langmuir* **2001**, *17*, 6720−6728.
(66) Tachibana, Y.; Moser, J. E.; Grätzel, M.; Klug, D. R.; Durrant, J. R. Subpicosecond Interfacial Charge Separation in Dye-Sensitized

DOI: 10.1021/acs.jpclett.8b02635
J. Phys. Chem. Lett. 2018, 9, 5810−5821

Nanocrystalline Titanium Dioxide Films. *J. Phys. Chem.* **1996**, *100*, 20056−20062.
(67) Lissau, J. S.; Nauroozi, D.; Santoni, M.-P.; Edvinsson, T.; Ott, S.; Gardner, J. M.; Morandeira, A. What Limits Photon Upconversion on Mesoporous Thin Films Sensitized by Solution-Phase Absorbers? *J. Phys. Chem. C* **2015**, *119*, 4550−4564.
(68) Gray, V.; Börjesson, K.; Dzebo, D.; Abrahamsson, M.; Albinsson, B.; Moth-Poulsen, K. Porphyrin−Anthracene Complexes: Potential in Triplet−Triplet Annihilation Upconversion. *J. Phys. Chem. C* **2016**, *120*, 19018−19026.
(69) Gray, V.; Dzebo, D.; Lundin, A.; Alborzpour, J.; Abrahamsson, M.; Albinsson, B.; Moth-Poulsen, K. Photophysical characterization of the 9,10-disubstituted anthracene chromophore and its applications in triplet-triplet annihilation photon upconversion. *J. Mater. Chem. C* **2015**, *3*, 11111−11121.
(70) Zhong, F.; Zhao, J. Phenyleneanthracene derivatives as triplet energy acceptor/emitter in red light excitable triplet-triplet-annihilation upconversion. *Dyes Pigm.* **2017**, *136*, 909−918.
(71) Gray, V.; Dreos, A.; Erhart, P.; Albinsson, B.; Moth-Poulsen, K.; Abrahamsson, M. Loss channels in Triplet-Triplet Annihilation Photon Upconversion: Importance of Annihilator Singlet and Triplet Surface Shapes. *Phys. Chem. Chem. Phys.* **2017**, *19*, 10931.
(72) Cheng, Y. Y.; Khoury, T.; Clady, R. G. C. R.; Tayebjee, M. J. Y.; Ekins-Daukes, N. J.; Crossley, M. J.; Schmidt, T. W. On the efficiency limit of triplet-triplet annihilation for photochemical upconversion. *Phys. Chem. Chem. Phys.* **2010**, *12*, 66−71.
(73) Auckett, J. E.; Chen, Y. Y.; Khoury, T.; Clady, R. G. C. R.; Ekins-Daukes, N. J.; Crossley, M. J.; Schmidt, T. W. Efficient up-conversion by triplet-triplet annihilation. *JPCS* **2009**, *185*, 012002.
(74) Hagstrom, A. L.; Deng, F.; Kim, J.-H. Enhanced Triplet−Triplet Annihilation Upconversion in Dual-Sensitizer Systems: Translating Broadband Light Absorption to Practical Solid-State Materials. *ACS Photonics* **2017**, *4*, 127.
(75) Klahr, B. M.; Hamann, T. W. Performance Enhancement and Limitations of Cobalt Bipyridyl Redox Shuttles in Dye-Sensitized Solar Cells. *J. Phys. Chem. C* **2009**, *113*, 14040−14045.
(76) Sommeling, P. M.; O'Regan, B. C.; Haswell, R. R.; Smit, H. J. P.; Bakker, N. J.; Smits, J. J. T.; Kroon, J. M.; van Roosmalen, J. A. M. Influence of a TiCl4 Post-Treatment on Nanocrystalline TiO2 Films in Dye-Sensitized Solar Cells. *J. Phys. Chem. B* **2006**, *110*, 19191−19197.
(77) Hagstrom, A. L.; Deng, F.; Kim, J.-H. Enhanced Triplet−Triplet Annihilation Upconversion in Dual-Sensitizer Systems: Translating Broadband Light Absorption to Practical Solid-State Materials. *ACS Photonics* **2017**, *4*, 127−137.
(78) Dzebo, D.; Moth-Poulsen, K.; Albinsson, B. Robust triplet−triplet annihilation photon upconversion by efficient oxygen scavenging. *Photochem. Photobiol. Sci.* **2017**, *16*, 1327−1334.
(79) Mehmood, U.; Al-Ahmed, A.; Al-Sulaiman, F. A.; Malik, M. I.; Shehzad, F.; Khan, A. U. H. Effect of temperature on the photovoltaic performance and stability of solid-state dye-sensitized solar cells: A review. *Renewable Sustainable Energy Rev.* **2017**, *79*, 946−959.
(80) Amemori, S.; Sasaki, Y.; Yanai, N.; Kimizuka, N. Near-Infrared-to-Visible Photon Upconversion Sensitized by a Metal Complex with Spin-Forbidden yet Strong S0−T1 Absorption. *J. Am. Chem. Soc.* **2016**, *138*, 8702−8705.
(81) Huang, Z.; Li, X.; Mahboub, M.; Hanson, K. M.; Nichols, V. M.; Le, H.; Tang, M. L.; Bardeen, C. J. Hybrid Molecule−Nanocrystal Photon Upconversion Across the Visible and Near-Infrared. *Nano Lett.* **2015**, *15*, 5552−5557.
(82) Wu, M.; Congreve, D. N.; Wilson, M. W. B.; Jean, J.; Geva, N.; Welborn, M.; Van Voorhis, T.; Bulović, V.; Bawendi, M. G.; Baldo, M. A. Solid-state infrared-to-visible upconversion sensitized by colloidal nanocrystals. *Nat. Photonics* **2016**, *10*, 31.
(83) Yanai, N.; Kozue, M.; Amemori, S.; Kabe, R.; Adachi, C.; Kimizuka, N. Increased vis-to-UV upconversion performance by energy level matching between a TADF donor and high triplet energy acceptors. *J. Mater. Chem. C* **2016**, *4*, 6447−6451.
(84) Peng, J.; Guo, X.; Jiang, X.; Zhao, D.; Ma, Y. Developing efficient heavy-atom-free photosensitizers applicable to TTA upconversion in polymer films. *Chem. Sci.* **2016**, *7*, 1233−1237.
(85) Wu, T. C.; Congreve, D. N.; Baldo, M. A. Solid state photon upconversion utilizing thermally activated delayed fluorescence molecules as triplet sensitizer. *Appl. Phys. Lett.* **2015**, *107*, 031103.
(86) Cao, L.; Wang, Y.; Zhong, J.; Han, Y.; Zhang, W.; Yu, X.; Xu, F.; Qi, D.-C.; Wee, A. T. S. Electronic Structure, Chemical Interactions and Molecular Orientations of 3,4,9,10-Perylene-tetracarboxylic-dianhydride on TiO2(110). *J. Phys. Chem. C* **2011**, *115*, 24880−24887.
(87) Moon, A. P.; Pandey, R.; Bender, J. A.; Cotton, D. E.; Renard, B. A.; Roberts, S. T. Using Heterodyne-Detected Electronic Sum Frequency Generation To Probe the Electronic Structure of Buried Interfaces. *J. Phys. Chem. C* **2017**, *121*, 18653−18664.
(88) Gundlach, L.; Szarko, J.; Socaciu-Siebert, L. D.; Neubauer, A.; Ernstorfer, R.; Willig, F. Different orientations of large rigid organic chromophores at the rutile TiO2 surface controlled by different binding geometries of specific anchor groups. *Phys. Rev. B: Condens. Matter Mater. Phys.* **2007**, *75*, 125320.
(89) Metoki, N.; Liu, L.; Beilis, E.; Eliaz, N.; Mandler, D. Preparation and Characterization of Alkylphosphonic Acid Self-Assembled Monolayers on Titanium Alloy by Chemisorption and Electrochemical Deposition. *Langmuir* **2014**, *30*, 6791−6799.
(90) Yazji, S.; Westermeier, C.; Weinbrenner, D.; Sachsenhauser, M.; Liao, K.-L.; Noever, S.; Postorino, P.; Schwartz, J.; Abstreiter, G.; Nickel, B.; Zardo, I.; Cattani-Scholz, A. Surface-directed molecular assembly of pentacene on aromatic organophosphonate self-assembled monolayers explored by polarized Raman spectroscopy. *J. Raman Spectrosc.* **2017**, *48*, 235−242.
(91) Lin, H.-C.; MacDonald, G. A.; Shi, Y.; Polaske, N. W.; McGrath, D. V.; Marder, S. R.; Armstrong, N. R.; Ratcliff, E. L.; Saavedra, S. S. Influence of Molecular Orientation on Charge-Transfer Processes at Phthalocyanine/Metal Oxide Interfaces and Relationship to Organic Photovoltaic Performance. *J. Phys. Chem. C* **2015**, *119*, 10304−10313.
(92) Zheng, Y.; Giordano, A. J.; Shallcross, R. C.; Fleming, S. R.; Barlow, S.; Armstrong, N. R.; Marder, S. R.; Saavedra, S. S. Surface Modification of Indium−Tin Oxide with Functionalized Perylene Diimides: Characterization of Orientation, Electron-Transfer Kinetics and Electronic Structure. *J. Phys. Chem. C* **2016**, *120*, 20040−20048.
(93) Wang, J. C.; Hill, S. P.; Dilbeck, T.; Ogunsolu, O. O.; Banerjee, T.; Hanson, K. Multimolecular assemblies on high surface area metal oxides and their role in interfacial energy and electron transfer. *Chem. Soc. Rev.* **2018**, *47*, 104−148.
(94) Balasingam, S. K.; Lee, M.; Kang, M. G.; Jun, Y. Improvement of dye-sensitized solar cells toward the broader light harvesting of the solar spectrum. *Chem. Commun.* **2013**, *49*, 1471−1487.
(95) Yakutkin, V.; Aleshchenkov, S.; Chernov, S.; Miteva, T.; Nelles, G.; Cheprakov, A.; Baluschev, S. Towards the IR Limit of the Triplet−Triplet Annihilation-Supported Up-Conversion: Tetraanthraporphyrin. *Chem. - Eur. J.* **2008**, *14*, 9846−9850.
(96) Englman, R.; Jortner, J. The energy gap law for radiationless transitions in large molecules. *Mol. Phys.* **1970**, *18*, 145−164.
(97) Freed, K. F.; Jortner, J. Multiphonon Processes in the Nonradiative Decay of Large Molecules. *J. Chem. Phys.* **1970**, *52*, 6272−6291.
(98) Kakiage, K.; Aoyama, Y.; Yano, T.; Oya, K.; Fujisawa, J.-i.; Hanaya, M. Highly-efficient dye-sensitized solar cells with collaborative sensitization by silyl-anchor and carboxy-anchor dyes. *Chem. Commun.* **2015**, *51*, 15894−15897.
(99) Yang, W. S.; Park, B.-W.; Jung, E. H.; Jeon, N. J.; Kim, Y. C.; Lee, D. U.; Shin, S. S.; Seo, J.; Kim, E. K.; Noh, J. H.; Seok, S. I. Iodide management in formamidinium-lead-halide−based perovskite layers for efficient solar cells. *Science* **2017**, *356*, 1376−1379.
(100) Charlton, J. L.; Dabestani, R.; Saltiel, J. Role of triplet-triplet annihilation in anthracene dimerization. *J. Am. Chem. Soc.* **1983**, *105*, 3473−3476.

DOI: 10.1021/acs.jpclett.8b02635
J. Phys. Chem. Lett. 2018, 9, 5810−5821

(101) Saltiel, J.; Atwater, B. W. Spin-Statistical Factors in Diffusion-Controlled Reactions. *Adv. Photochem.* **2007**, *14*, 1.
(102) McLean, A. J.; Truscott, T. G. Faraday communications. Efficiency of triplet-photosensitised singlet oxygen generation in benzene. *J. Chem. Soc., Faraday Trans.* **1990**, *86*, 2671−2672.
(103) Bachilo, S. M.; Weisman, R. B. Determination of Triplet Quantum Yields from Triplet−Triplet Annihilation Fluorescence. *J. Phys. Chem. A* **2000**, *104*, 7711−7714.
(104) Hoseinkhani, S.; Tubino, R.; Meinardi, F.; Monguzzi, A. Achieving the photon up-conversion thermodynamic yield upper limit by sensitized triplet−triplet annihilation. *Phys. Chem. Chem. Phys.* **2015**, *17*, 4020−4024.
(105) DeRosa, M. C.; Crutchley, R. J. Photosensitized singlet oxygen and its applications. *Coord. Chem. Rev.* **2002**, *233*−*234*, 351−371.
(106) Diffey, B. Solar Spectral Irradiance and Summary Outputs Using Excel. *Photochem. Photobiol.* **2015**, *91*, 553−557.

DOI: 10.1021/acs.jpclett.8b02635
J. Phys. Chem. Lett. 2018, 9, 5810−5821